Life Science Informatics Publications

Research Journal of Life Sciences, Bioinformatics, Pharmaceutical and Chemical Sciences

Journal Home page http://www.rjlbpcs.com/

RJLBPCS

ISSN 2454-6348

Original Research Article **DOI: 10.26479/2024.1001.05**

NOVELTY AND CHARACTERIZATION OF MICROTUBULE ASSOCIATED PROTEIN INVOLVED IN CELLULOSE BIOSYNTHESIS

N. Sasirekha[1], M. Mumtaz[2], K. Manimegalai[3], P. Sheela[4], M. Karthigeyan[5]

1. Department of Zoology, Government Arts College for Women, Sivagangai.
2. Department of Zoology, M.S.S. Wakf Board College, Madurai.
3. Department of Zoology, Sri GVG Visalakshi College for Women, Udumalpet.
4. Department of Botany, V. O. Chidambaram College, Thoothukudi.
5. Department of Zoology, Arumugam Pillai SeethaiAmmal College, Tiruppattur, Sivagangai.

ABSTRACT: Cell walls are a distinct feature of plants and their chemical constituents, cellulose, hemicelluloses and lignin, are economically valuable. Plant fibres rich in cellulose, which mainly resides in their cell wall, are traditionally used in making paper and textiles. The changing global economic situation and environmental concerns have imparted necessity for renewable, but at the same time value added cellulosic materials. Characterization of these genes will potentially give additional opportunities to modify fibre properties. This paper discussthe discovery and characterization of a highly upregulated gene with a previously unknown function in poplar xylem, here denoted *Ptt*MAP20.All the results obtained so far indicate that *Ptt*MAP20 is a novel microtubule associated protein that binds to a cellulose biosynthesis inhibitor, DCB (2,6-dichlorobenzonitrile) and is required during cellulose biosynthesis in secondary cell walls.The general objective of the present investigation was to characterize a gene ofunknown function that was found to be highly expressed during the secondary cellwall formation in *Populustremula*× *Populustremuloides*(hybrid aspen).

Keywords: MAP (Microtubule Associated Protein), unknown gene, cellulose biosynthesis, *Populus*, microtubule, DCB

Article History: Received: Dec 20, 2023; Revised: Jan 06, 2024; Accepted: Jan 15, 2024.

Corresponding Author: Dr. N. Sasirekha* Ph.D.
Guest Lecturer, Department of Zoology, Government Arts College for Women, Sivagangai.
E-mail Address: smartsasi12@gmail.com

1. INTRODUCTION

Cellulose is a linear organic polymer made up of glucose units. It is the main constituent of the cell walls (or the extracellular matrix) of all land plants, higher algae, oomycetes and some bacteria. Cellulose is the most abundant organic material in nature and represents a renewable, biodegradable, biocompatible and derivatisable natural raw material for various industrial uses. Cellulosic materials have contributed to the development of human life in many ways. Paper is still the main material used globally to disseminate information and knowledge and to provide raw material for packaging and household uses. The longfibres from softwood (conifers) and short fibres from hardwood (deciduous) trees determine the strength, opacity and surface smoothness of paper. Softwood trees such as spruce, pine, fir, larchand hemlock and hardwood trees such as eucalyptus, aspen and birch are extensively used to extract pulp [1-7].Starch was used as the biomass in the past but cellulose is slowly replacing it. As early as 1838, Payen coined the name cellulose [8-13]. Cellulose is an unbranched polymer of glucopyranose units joined by β-(1,4)linkages.

2. MATERIALS AND METHODS

Transcript Profiling

Expression data from microarray experiments were obtained from UPSCBASE (www.upscbase.db.umu.se), experiment number 30 (courtesy of GöranSandberg) using the following PU numbers *PttCS1*: PU07560; *PttCS3*: PUPU07525,PU07543, PU30161 (mean values); *PttCS*9: PU06755; *Ptt*MAP20: PU00458,PU02741. The data was normalized against a sample containing equal amount ofRNA from all tissues and organs analyzed.

Quantitative PCR

Stem samples from *P. tremula* were collected from a natural population of ca5 m high trees growing outside Umeå, immediately frozen in liquid nitrogen andstored at -70°C. Total RNA extraction, cDNA synthesis and SYBR green qPCR were performed using Bio-Rad Aurum Plant Mini Kit, Bio-Rad iScript cDNA synthesis kit and Bio-Rad SYBRGreen qPCR mix respectively following manufacturer's instructions. All qPCR data was expressed as –ΔCt values (where ΔCt is CtCONTROL GENE - CtTEST GENE). The data were normalized by using two housekeeping genes, ubiquitin (Pt794626,fgenesh4_pg.C_scaffold_13026000001) and elongation factor 1β (Pt815174,estExt_fgenesh4_pg.C_LG_I1178). Mean Ct values for these two genes were used when calculating ΔCt values. Each sample was analyzed in 3 technical replicates. Primers used for gene expression analysis were designed from *P. trichocarpa*gene model sequences. The PCR program

included initial denaturation at 95°C for 3 min; 40 cycles of 10 s at 95°C, 30 s at 55°C,30 s at 72°C and a final melt curve analysis (incremental heating from 54°C to 95°C).

Phylogenetic analysis

Phylogeny studies were done using Mr Bayes [14]. Each analysis had four MCMC chains running for 4x106 iterations, default thinning and the first 10% iterations removed as burn in. The mixed amino acid model with gamma-distributed rate-change over sites was chosen. Analysis of possible adaptive evolution was performed with codeml in the PAML package [15]. The gene mapping is explained hereafter.

Gene mapping

Mapping of the transcripts or proteins to genome sequences and the determination of exon/intron-structure was done using Exonerate [16]. Promoter analyses were conducted using TSSP [17]. Phylogenetic foot printing for motif finding was done with MEME with settings chosen to look for up to five motifs, present in some but not necessarily all sequences. Local genomic alignments were computed using DBA [18].

Expression profiling of TPX2 genes in Arabidopsis

The expression profiling data for the *Arabidopsis* TPX2 genes were extracted from the Gene Atlas performed with ATH1 (22K full genome Arabidopsis Affymetrix GeneChip) available online (http://www.arabidopsis.org/).Antibodies were raised against the full length *Ptt*MAP20 protein expressed in *E.coli* using the expression vector pAFF8c-3c encoding N-terminal polyHis6 and albumin binding domain (ABP) tags in frame with the inducible T7 promoter [19].

The full-length cDNA sequence was cloned using the following primers:

forward 5'-GCAGATACAGCGGCCGCAATGGGAAAGCACACAAAAATCTG-3' and reverse 5'-GGCGGCGCGCCTTAATTAACAGCTTCCAGGCATGATC-3',followed by insertion into the poly-cloning site of pAff8c-3c and transformation and expression in *E. coli* BL 21-CodonPlus (DE3)-RIL (Stratagene).

Protein expression was carried out as described by [19], followed by purification of there combinant protein under denaturing conditions using the polyHis6 tag using TALONspin™ (BD Bioscience, Mumbai) columns following the manufacturer's recommendations. The homogenized slurry was centrifuged at 4000g for 20 min at 4°C and the resulting supernatant was used as the crude extract of essentially soluble proteins (referred to as the supernatant). The protein concentration in the supernatant was measured using the BioRad Protein assay (BioRad Laboratories, Mumbai) with BSA as standard.

Co-precipitation assay of binding of PttMAP20 to poplar MT

PMT were obtained by *in vitro* assembly of tubulin monomers contained in50µg of xylem protein extract (supernatant fraction) following the instructions of the spin down assay kit BK029 of Cytoskeleton Inc. In brief, to assemble aspen microtubules, 20 µl of the xylem protein extract

(supernatant fraction, 9.4 µg / µl) was mixed with 2.5 µl of the Cushion Buffer (BK029, Cytoskeleton) and incubated at 35°C for 20 min. The synthesized PMT were then stabilized and diluted with 200 µl of the pre-warmed general tubulin buffer (BK029, Cytoskeleton), supplemented with 10 µl of taxol, at 35° C for 30 min.

Assembly of BMT in the presence of DCB

100 µg batches of monomeric α and β tubulins in 20 µL of the GeneralTubulin Buffer (Cytoskeleton, Mumbai) were mixed with increasing concentrations of DCB (0.75 µM –7500 µM) dissolved in DMSO and incubated on ice for 10 min. Afinal concentration of 10 mM GTP was then added to initiate polymerization of BMT, followed by analysis of the extent of polymerization using the MT Binding Protein Spin Down Assay Kit (Cytoskeleton, Mumbai).

Confocal microscopy, tobacco

Confocal microscopy was performed 3-5 days after agro infiltration on a Zeiss Confocal microscope, LSM 510 META. Sections of leaves were mounted on slides ina water/glycerol solution. Images were acquired with an argon/krypton laser. Images were acquired with the following settings for the microscope: For YFP, excitation of laser line 514 nm, emission filter BP 530-600 nm using a Plan-Apochromat 63x/1.4oil objective lens.PCR products were cloned into Gateway pENTR/D-TOPO vector using the directional TOPO cloning kit (Invitrogen), according to the manufacturer's instructions. MAP20 ORF was then recombined using the Gateway LR ClonaseEnzyme Mix (Invitrogen) into the destination vectors pEarley Gate 101 and 104 to create a C-terminal and N-terminal fusion, respectively. All the *Agrobacterium* strains harboured the pCH32 helper plasmid [21].

Transmission electron microscopy (TEM), poplar tissues

Developing wood tissue segments of Poplar trees (*P. tremula*X *P. tremuloides*clone T89) cultivated under natural light in the green house to a height of 5 m were dissected from the stems [21]. The tissue samples were pre-treated with 6 M urea for 60 min [22], washed 3 times for 10 min with 25 mM potassium phosphate buffer (pH 7.2), fixed overnight at 4°C in 4% (v/v) paraformaldehyde, 0.05% (v/v) glutaraldehyde in 25 mM phosphate buffer and washed again 3 times for 10 min with the buffer. The samples were then dehydrated through a graded ethanol series (50%, 70%, 80%, 90%, 95% and 99.5%) 3 times in each, for 10 min. LRW resin (TAAB Laboratories, Reading, Mumbai) was then added dropwise to absolute ethanol to reach a final concentration of 10% and the infiltration of resin was performed overnight. This was followed by one 50% and two 100%LRW changes and overnight infiltration step for each change. The material was transferred to the gelatin capsules and polymerized for 8-24 hrs at 60° C.

Phenotypic Characterization-Overexpression of PttMAP20 in Arabidopsis

In order to generate transgenic *Arabidopsis* plants overexpressing *PttMAP20*fused to the myc epitope at the C-terminus with the 35S promoter, wild type ecotypes (Col-0) were transformed using

the floral dip method and selected on kanamycin-containing media. Transformation was verified by phenotype and PCR analysis using primers specific for *PttMAP20*. The expression was verified by RT-PCR carried out as follows. Total RNA was isolated from poplar leaf, xylem and phloem tissues using RNeasy plant minikit from Qiagen and 0.2 micrograms was used for RT-PCR using SuperScript III from Invitrogen. The following primers were used for *Ptt*MAP20detection: N-NO-TPX2 forward (5'-CACCATGGAGAAAGCACACACA-3'), N-NOTPX2reverse (5'-TTTGAATTCCTGGGGCTTAGTG-3'). The housekeeping ribosomalRNA gene (23S-40S) was used as a reference: 23S-40S forward (5'-CTGGTCGCAAGCTCAAGTCCCAC-3') and 23S-40S reverse (5'-GACCTTGGCTTCTCCTTCTTCTCTTTG-3').

3. RESULTS AND DISCUSSION

Discovery and Expression Analysis of Pttmap20

Data from microarray analysis of different poplar tissues and organs show that a small cytosolic protein is preferentially expressed in developing secondary xylem tissues (Figure 1A). This gene was denoted Unk1 but was later renamed *Ptt*MAP20. The new name will be used throughout the thesis. The expression pattern of *Ptt*MAP20 is remarkably similar to three previously identified xylem associated *PttCESA*genes [23].

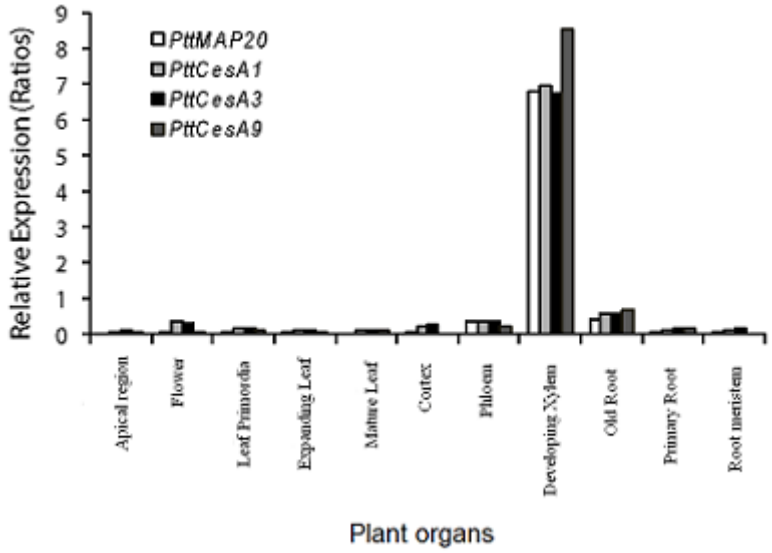

Figure 1A Co-expression of poplar secondary cell wall associated *CESA* genes and *MAP20.*

Relative mRNA abundance of *PttCESA1*, *PttCESA3*, *PttCESA9* and *PttMAP20* in different tissues and organs as analyzed on cDNA microarrays.To confirm this pattern of expression, high-resolution quantitative PCR expression analysis (qPCR) of *PtMAP20* and *PtCESA1, PtCESA3-2 and PtCESA9-2* was conducted across the wood forming tissues. Tissue samples were dissected into 8 fractions from functional phloem towards maturing wood cells using tangential cryosectioning [20] giving a spatial resolution of gene expression of about 90µm in the radial direction (Figure 1B, side panel). Indeed, *PtMAP20* expression was very low in functional phloem tissues and primary walled cambial cells while it increased in expanding cells and most dramatically at the onset of secondary

wall biosynthesis (Figure 1B). The peak values of *PtMAP20* expression in fractions 4 - 6 corresponded to the peak rate of fiber wall thickening as measured from SEM images of the corresponding tissue.

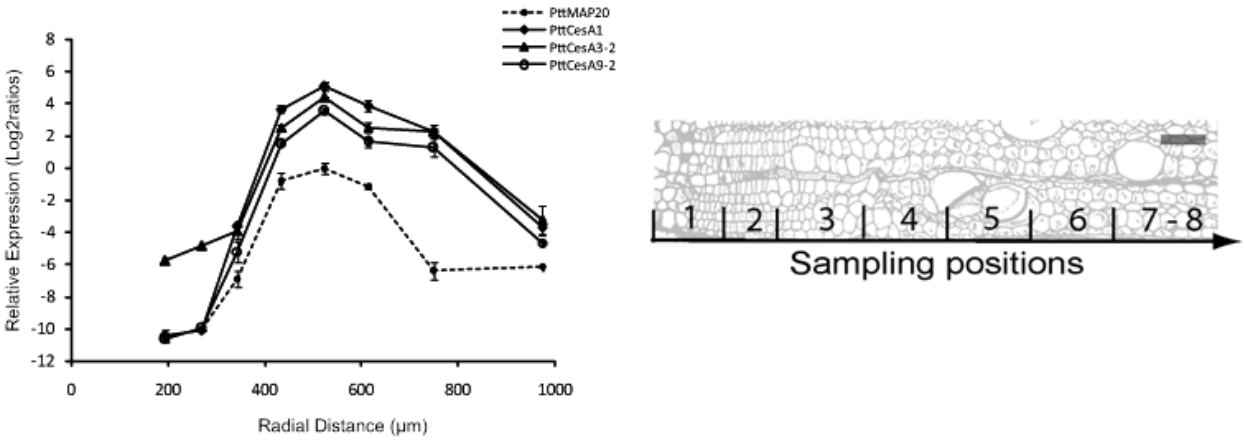

Figure 1B The relative mRNA abundance of *PtCESA1*, *PtCESA 3-2*, *PtCESA 9-2* and *PtMAP20* as quantified by qPCR in eight samples across developing xylem tissues, from functional phloem towards maturing wood cells.

The approximate sampling positions are indicated on an anatomical section as follows: functional phloem (1), cambial meristem (2), expanding wood cells (3) secondary cell wall forming and maturing wood cells (4-8). Scale bar =50µm.

The identity or similarity to a consensus sequence is indicated in blue and red (respectively), the last codon of an exon in orange and the exon/intron boundary in frame 2 in yellow.

Phylogenetic analysis of TPX2 domain

Probabilities exceeding 0.8 were removed for clarity. The clades with M20L proteins and KLEEK motif are marked. Mutations in genes with reported phenotypes in *Arabidopsis* are marked in red.

Molecular evolution of the TPX2 domain was studied with phylogenetic analysis of all available TPX2 domain sequences. The subtrees in the phylogeny mostly follow the established species history (Figure 3A), but there are peculiarities to note.

The TPX2 domain is marked with a black bar and the extended TPX2 domain by a dotted line under the sequences. Notes above the TPX2 domain indicate sites where residues are lost relative to the Pfam domain model of TPX2.

The lack of phylogenetic resolution is seen also in other parts of the tree, including several branches with low statistical support. The M20L clade was revisited by reconstructing a phylogeny based on all Angiosperm extended TPX2 domains of M20L whereby the branching was significantly improved (Figure 3B).

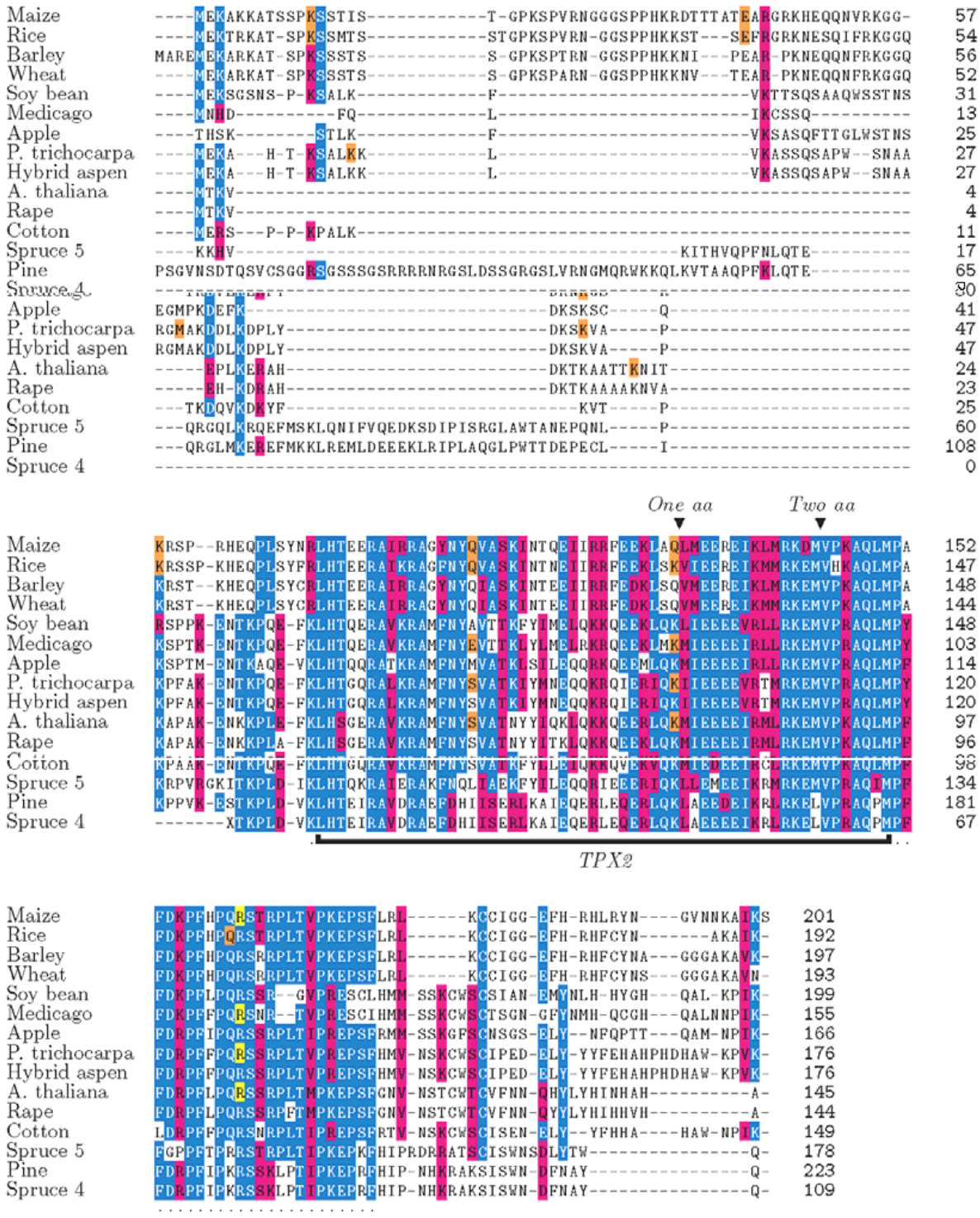

Figure 2 Sequence alignment of M20L proteins made with the MAFFT alignment tool.

The phylogenetic tree has two distinct branches, one for animals and one for plants. Proteins containing a KLEEK motif form a monophyletic clade and have several branches each with its own monocot and dicot sub-branches, as exemplified by WDL5/WDL6 and WDL4 in Figure 3A. Based on our current analysis the M20L genes constitute a clade in the non-KLEEK branch.

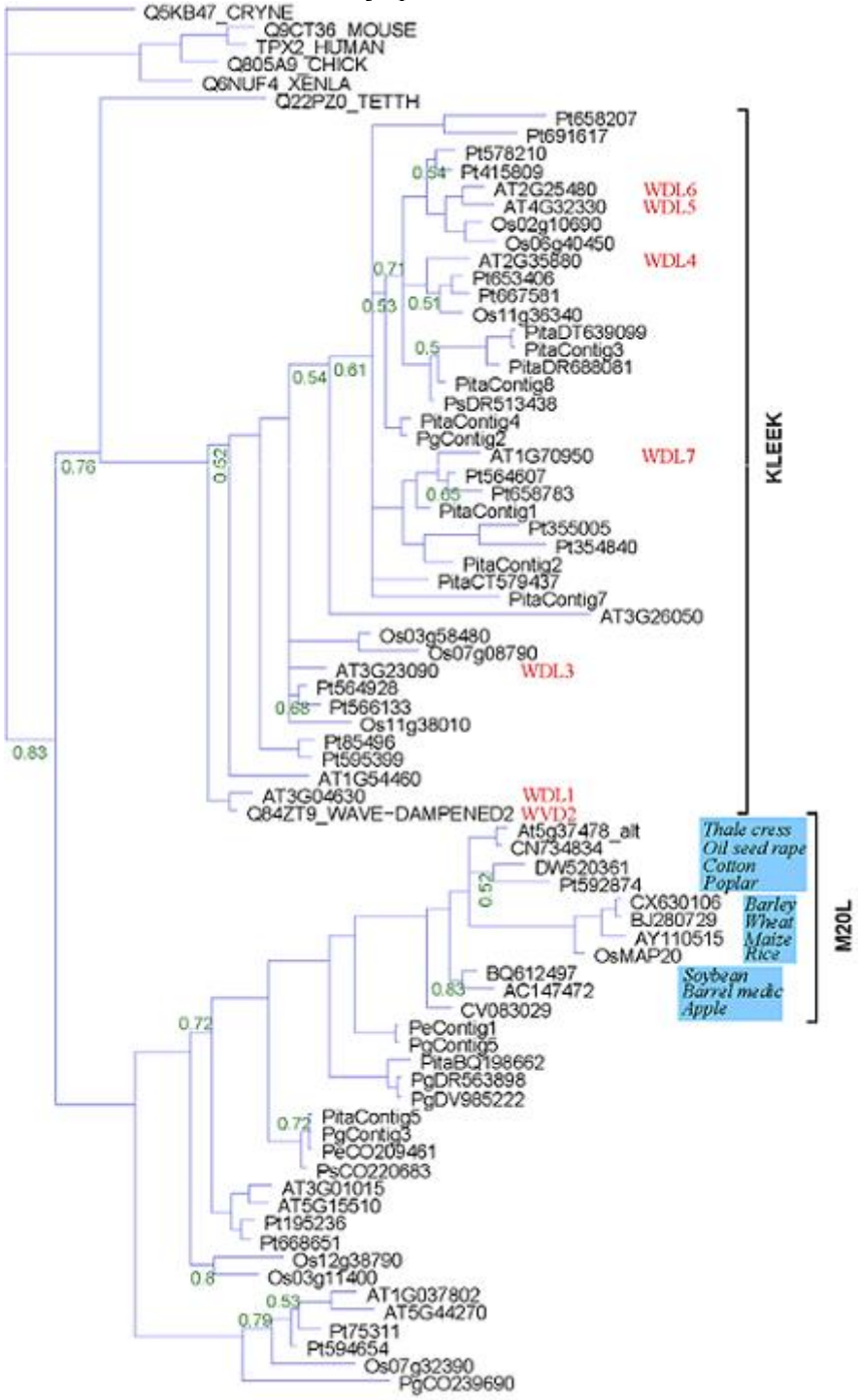

Figure 3A Phylogenetic tree made with all the available and newly found eukaryotic proteins containing a TPX2 domain. The Bayesian posterior probability is indicated for weak branches.

Notice that gymnosperm sequences are present in both major branches and that there are two likely orthologs to *Ptt*MAP20 in *Picea*. Secondly, *Tetrahymenathermophila*is found in the plant clade, adjacent to the KLEEK-containing proteins, which is not reasonable given the species tree. Again this could be due to lack of data, but there is also another interpretation: If *T. thermophila*is considered an out group of the present phylogeny, i.e. we re-root the tree at the base of the *thermophila* branch, then the first duplication occurred before plants and animals diverged. This

implies that animals lost at least one TPX2 gene, while plants took advantage of the redundancy by further evolutionary diversification.

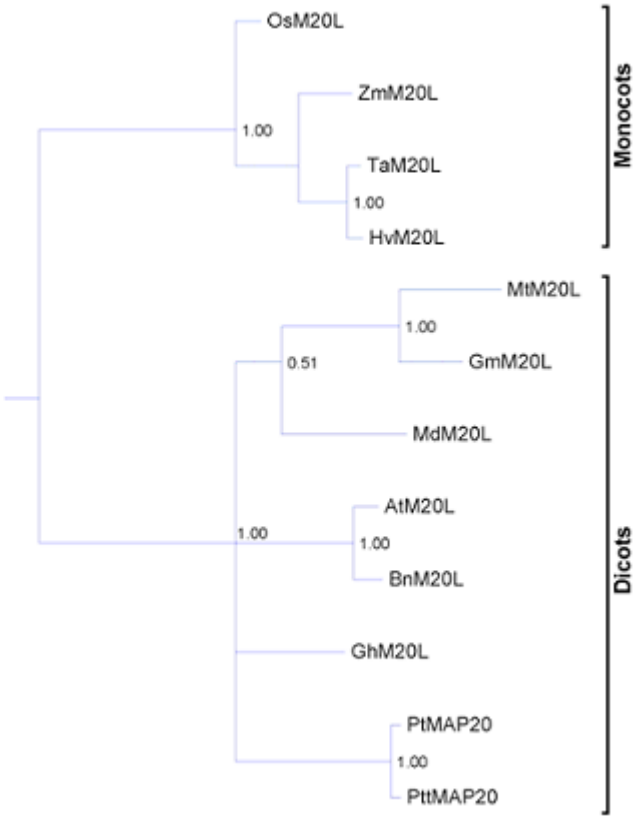

Figure 3B Phylogenetic tree made with extended TPX2 domain.

Genomic organization of TPX2 genes

The organization of TPX2 genes was mapped in all the three fully sequenced model plants: the universal model *Arabidopsis*, the wood model *Populus*and the grass model *Oryza*. We could not find a general pattern for the TPX2 gene locations in the three genomes (Figure 4A and B). Synteny comparisons suggested that many recent paralogs, e.g. WDL1/WVD2 and WDL6/WDL5 in our phylogeny, could be due to large scale duplications (Table 2). The linkage groups previously found in the three species were used to overlay the location of these gene pairs [24-26].

The many recent paralogs, especially in Poplar, could make the gene localization ambiguous, but the highest scoring alignment stood out in cases. All genes in the TPX2 gene family in *P. trichocarpa*, except *MAP20*, seem to come in pairs and they are all more recent than the last species split in this phylogeny. While there are plenty of duplications in the TPX2 gene family in general, none of the species included in the present study has more than a single copy of *M20L* genes.

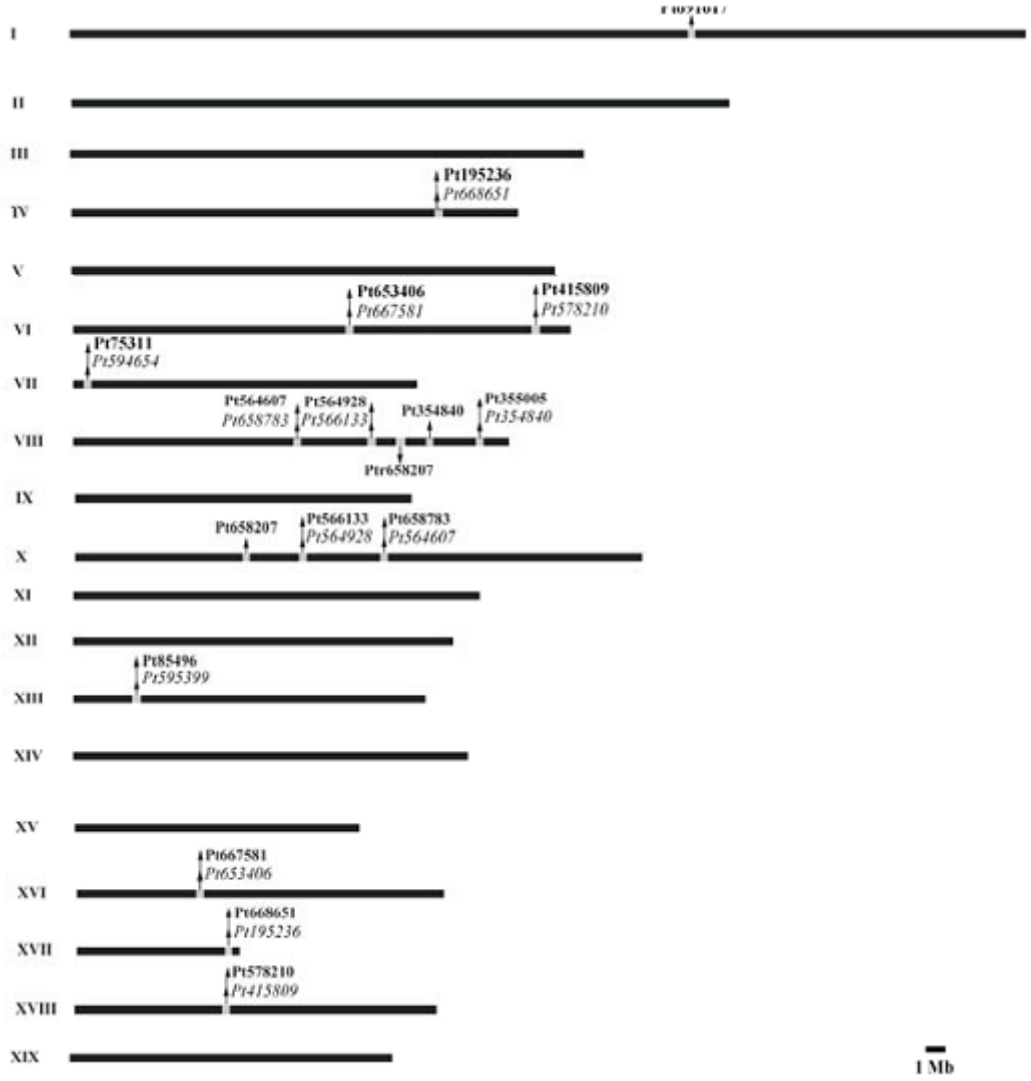

Figure 4A Genomic organization (to scale) of TPX2 genes in the genome of *Populustrichocarpa*

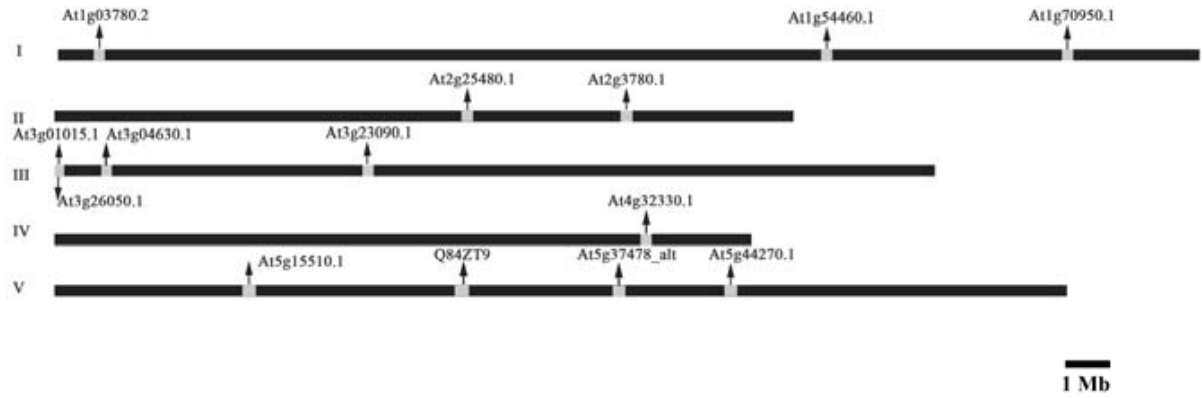

Figure 4B Genomic organization (to scale) of TPX2 genes in the genome of *Arabidopsis thaliana*.

Microarray experiments in *Arabidopsis* indicate that WDL1 (At3g04630) and WVD2 (At1g3780) have similar expression patterns (Figure 2) with increased expression in inflorescence tissue,

consistent with a duplicated regulatory module. Even WDL5 (At4g32330) exhibits somewhat increased expression in inflorescence tissue.

Bioinformatic Characterization

Identification and sequence analysis of PttMAP20 orthologs

The cDNA clone, used in the microarrays experiments, of *Ptt*MAP20 encoded the full length gene. At the initial phase of the discovery, the *Ptt*MAP20 sequence blast analysis didn't yield any hit. The protein sequence was predicted to be a soluble coiled coil. The TPX2 domain in the *Ptt*MAP20 protein sequence was revealed in the blast searches only later. Due to the possible involvement of *Ptt*MAP20 in cellulose biosynthesis, putative orthologs (as defined by Fitch, 1970) were searched for corresponding genes in all published plant genomes and in the NCBI dbEST (Table 2).

Table 1 Gene pairs and their respective linkage groups present in *Populustrichocarpa, Oryza sativa and Arabidopsis thaliana*

Species	Duplicated gene pairs	Linkage group
Populustrichocarpa	Pt668651: Pt195236	IV: XVII
	Pt415809: Pt578210	VI: XVIII
	Pt658783: Pt564607	VIII: X
	Pt667581: Pt653406	VI: XVI
	Pt658207:Pt658207	VIII:X
Oryza sativa	Os02g10690.1: Os06g40450.1	II: VI
	Os03g58480.1: Os12g38790.1	III: XII
Arabidopsis thaliana	AT2g25480.1: At4g32330.1	II: V
	Q84ZT9: At3g04630.1	III:V

The current annotations of the gene models Os09g13650.1 in rice and At5g37478 in *A. thaliana* had to be adjusted since sequences homologous to the other TPX2 proteins were detected beyond the current gene models (see Materials and Methods).

Reannotation of the rice gene was facilitated by an EST sequence, NM_001069361.1 and in both cases the new gene models were more similar to *PttMAP20* than the current gene models. Table 2 summarizes the gene models identified in different plant species.

Multiple alignments of the MAP20-like proteins were computed using MUSCLE, MAFFT and KALIGN, but no reliable full-length alignment could be found. In particular, there was little consensus at the N- and C-terminal ends of the proteins (see Figure 2 and Figure 1 for MAFFT and MUSCLE alignments, respectively).

Biochemical Characterization

Antibody development and recombinant expression in *E. coli*

Polyclonal antibodies were raised in rabbits using recombinant *Ptt*MAP20fused to an albumin-binding protein. In Western blot analysis the resulting antibodies were found to recognize

specifically the recombinant *Ptt*MAP20 while a single protein band of slightly higher molecular mass (33kD) was detected in crude protein extracts from developing xylem (Supplemental Figure 5A).Since similar discrepancies between the predicted molecular weight and protein mobility in SDSPAGE have also been observed for other MAPs [27, 28], since no other cross reacting bands were recognized in the plant protein extract and since the antibody clearly recognized the recombinant *Ptt*MAP20, the antibody was considered specific for *Ptt*MAP20.

Table 2 A list of MAP20-Like gene models (*M20L*) in different plant species

Species	Accession	Origin	Protein acc
Populustrichocarpa	eugene3.00440209 (592874) (denoted estExt_ fgenesh4_ pg.C _440200 in the Populus genome release 1.1)	Gene prediction	*Pt*MAP20
P. tremula x P. tremuloides	POPLAR.3073.C1	PopulusDB	*Ptt*MAP20a
Arabidopsis thaliana	At5g37478	Gene prediction	*At*M20L At5g37478_altb
Oyza sativa	Os09g13650.1	Gene prediction	*Os*M20Lb
Medicagotruncatula	AC147472	Genome scaffold	*Mt*M20L
Brassica napus	CN734834	dbEST	*Bn*M20L
Gossypiumhirsutum	DW520361	dbEST	*Gh*M20L
Glycine max	BQ612497	dbEST	*Gm*M20L
Hordeumvulgare	CX630106	dbEST	*Hv*M20L
Malusdomestica	CV083029	dbEST	*Md*M20Lc
Triticumaestivum	BJ280729	dbEST	*Ta*M20L
Zeamaise	AY110515	dbEST	*Zm*M20Ld

a Identical to *Pt*MAP20; b New gene model; c Single EST support, may be short on 5' side; d Ambiguous codons were resolved using the shorter AI795385.

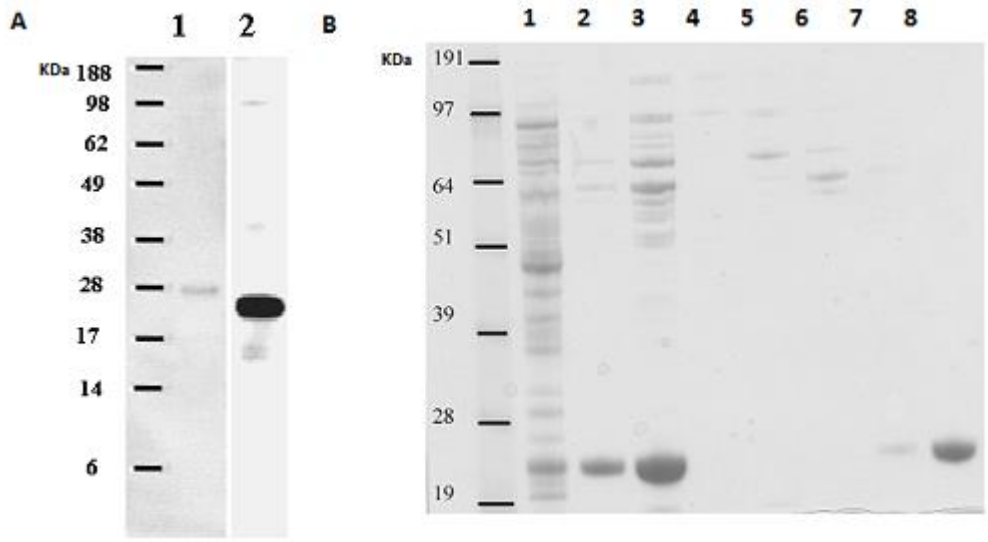

Figure 5 A. *Ptt*MAP20 in poplar tissue extracts as detected using *Ptt*MAP20 specific antibodies in a Western blot. Left lane, SeeBlue® Plus2 prestained protein standard (LC5925, Invitrogen); lane 1 - xylem extract; lane 2- recombinant *Ptt*MAP20 protein.
B. SDS-PAGE analysis of recombinant *Ptt*MAP20 expressed in *E. coli* during different stages of purification. MWL - SeeBlue® Plus2 pre-stained protein molecular weight standard (Invitrogen); lane 1, total soluble protein extract of *E. coli* cells expressing*Ptt*MAP20; 2, *Ptt*MAP20 protein eluted from the Ni Sepharose™ High performance matrix; 3, the same sample as in lane 2 after concentration and buffer exchange; lanes 4 – 8, fractions eluted from HiLoad16/60 Superdex 75pg size exclusion matrix. Lanes 4 – 7, 20µL of protein sample; lane 8, 1µg of representative fraction of purified *Ptt*MAP20.

PttMAP20-MT binding studies

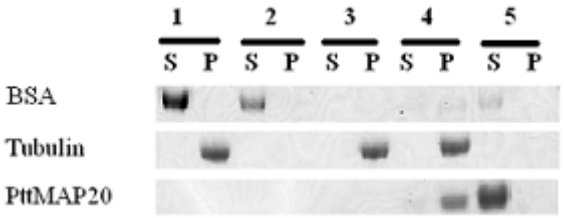

Figure 6A Coomassie blue stained SDS-PAGE (color inverted) demonstrating the binding of*Ptt*MAP20 to bovine microtubules (BMT) *in vitro.* 20 µL of supernatant (S) or 5 µL of resuspended pellet (P) (see text) containing the different proteins were loaded in the gel as follows: 1. BSA and BMT; 2.BSA; 3. BMT; 4. BMT and *Ptt*MAP20; 5. *Ptt*MAP20.

Images are shown of *in vitro* assembled PMT and BMT incubated with no *Ptt*MAP20 (A3, D3), with xylem extract containing *Ptt*MAP20 (B3, E3) and with recombinant *Ptt*MAP20 (C3 and F3). Columns A1-C1 and D1-F1 detection of the assembled PMT and BMT respectively by using visible light; columns A2-F2 detection of the mouse anti-α-tubulin antibodies labelled with Rhodamine (TRITC)-conjugated affinity-pure rabbit anti-mouse IgG antibodies; columns A3-F3 detection of

anti-*Ptt*MAP20 antibodies labeled with anti-rabbit Alexa Fluor®-488-fluoro-nanogold™ Fab fragment; columns A4 – G4, an overlay of the images in columns 2 and 3;

Control lane G experiment performed without including MT but rest of other components as in lane C and F.

The presence of a TPX2 domain suggested that *Ptt*MAP20 might be a microtubule associated protein. To test this hypothesis, *Ptt*MAP20 was expressed in*E. coli*, purified (Figure 6B) and used for binding studies with *in vitro* polymerizedbovine microtubules (BMT).

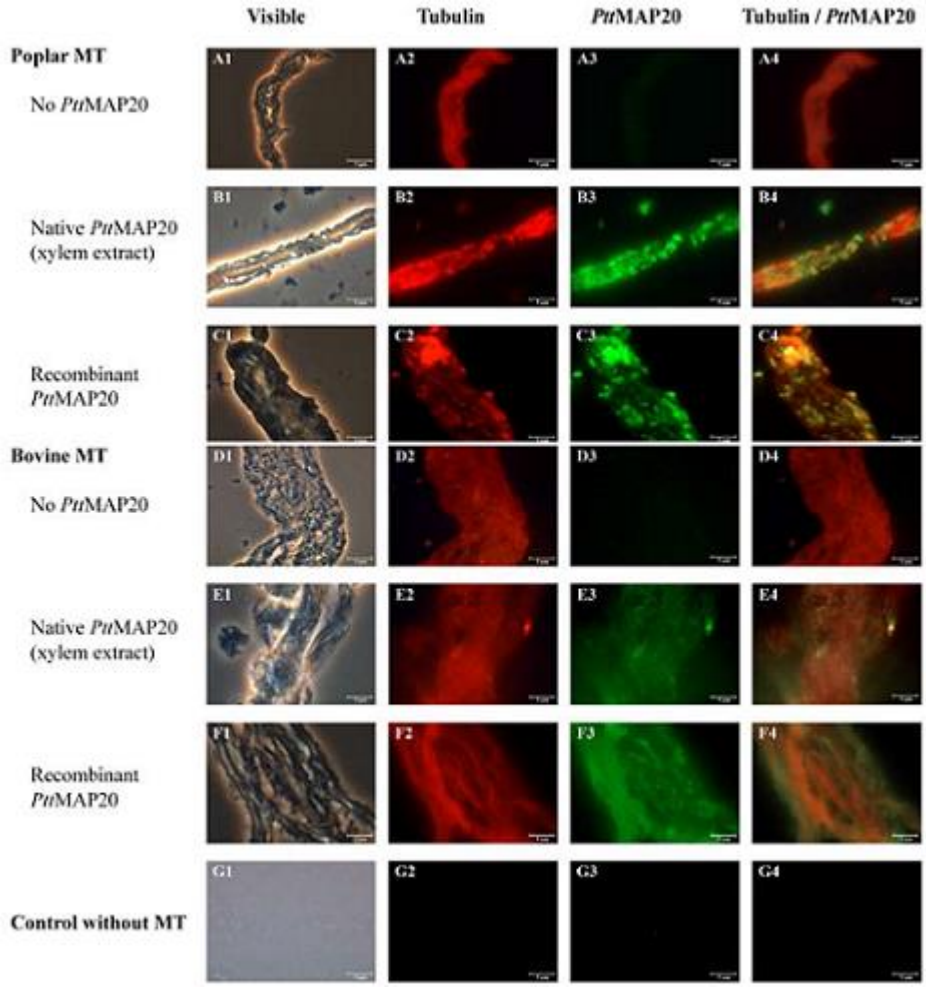

Figure 6B Fluorescent micrographs showing the binding of *Ptt*MAP20 onto poplar and bovine MT.

After incubation with BMT and centrifugation, *Ptt*MAP20 was recovered in the pellet fraction together with BMT (Figure 6A lane4P), while it remained in the supernatant fraction in the absence of BMT (Figure 6A,lane 5S). BMT in the absence of other proteins were found in the pellet (Figure 6A,lane 3P) while BSA (used as a non-binding control protein) remained in the supernatant, whether incubated with or without BMT (Figure 6A, lanes 1S and 2S,respectively). These data indicate that *Ptt*MAP20 indeed binds to microtubuli.

Phenotypic Characterization

Overexpression in Arabidopsis

Stable *Arabidopsis* plants expressing *PttMAP20* under the CaMV 35Spromoter were generated and the overexpression was confirmed by real time PCR (Figure 7A). Inspection of the visual phenotypes of several independent overexpressing (OE) lines revealed left-handed helical growth of rosettes leaves (Figure 7B) and stunted root growth (Figure 7C), two phenotypes that have been previously observed with microtubule destabilization [29, 30].

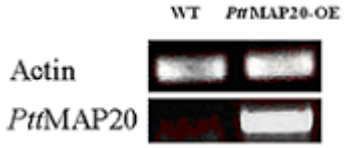

Figure 7 Preliminary characterization of transgenic lines of *Arabidopsis* overexpressing *Ptt*MAP20 (A) RT-PCR analysis of wild type (WT) and transgenic (*Ptt*MAP20-OE) plants using primers specific for*Ptt*MAP20 and Actin.

DISCUSSION

The economic importance of cellulose has imparted enormous scope for its research. The discovery and characterization of *Ptt*MAP20 is one such example. The *PttMAP20* gene was first discovered in a microarray experiment performed to expression profile the wood formation process in hybrid aspen. Bioinformatic analyses showed that *Ptt*MAP20 asa gene of unknown function had no hit in blast searches and it encoded a cytosoliccoiled coil protein. At transcript level the expression pattern of *Ptt*MAP20 was found to follow the secondary cell wall specific CESA genes. The original TPX2protein sequence contains two short domains predicted to adopt a coiled coil structure often involved in protein-protein interactions, one at the N-terminus (residues 171-208) and one at the C-terminus (650-684). The C-terminal coiled coil domain ishighly conserved in all TPX2-like proteins and it is thus called the TPX2 domain. Proteins containing a TPX2 domain have so far been identified in animals, fungi and plants but functional data concerning these proteins is scarce. Animal TPX2 is reported to interact with proteins using microtubules as a landing place to perform their function [31, 32].However, a common origin is apparent for the TPX2 domains suggesting that these domains share a similar function. Only the extended TPX2 domain was studied since we could not derive a reliable multi alignment over the full protein sequences. The hypothesis was that key properties in this conserved region could have changed, especially after themonocot/dicot split. However, no signs of positive selection were found, either over branches or on sequence sites. The extended TPX2 domain thus seems to have been under negative selection only.

4. CONCLUSION

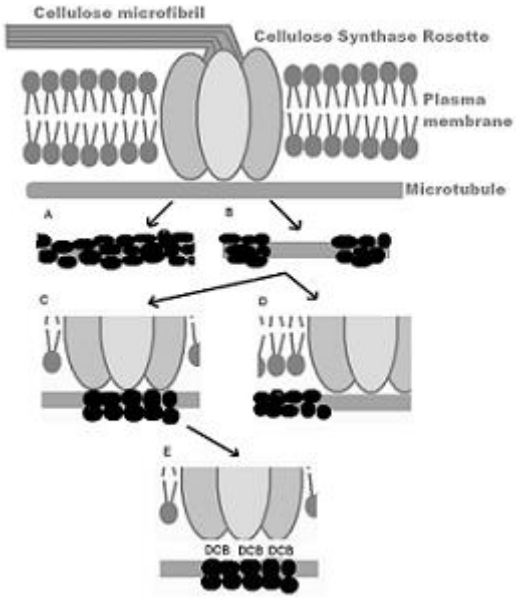

Figure 8 A cartoon illustrating possible molecular functions of *Ptt*MAP20.

A. *Ptt*MAP20 has been shown to bind microtubuli*in vitro* and *in vivo*.

Hypothesis 1: Targeting of *Ptt*MAP20 and binding of it to microtubule might be regulated by phosphorylation by kinases that are specific for each phase of cellular development.

B. *Ptt*MAP20 is found as patches *in situ* and also *in vivo*.

Hypothesis 2: The patches might be formed by the change or microtubule filament surface which could be due to its contact with other organelles or its polymerizing and depolymerizing ends.

C. Hypothesis 3: The patches could be an indication of a direct or indirect association of *Ptt*MAP20 to a protein complex example CesA complex.

D. Hypothesis 4: The patches of MAP20 might be guiding the contact of the rosettes with microtubule without itself having a direct binding to the rosette.

E. *Ptt*MAP20 binds to DCB but DCB doesn't affect the binding of *Ptt*MAP20 to microtubuli and microtubuli polymerization.

Hypothesis 5: This is possible if hypothesis 3 is valid. *Ptt*MAP20 - when bound to DCB - might loose its contact with the Ces A complex and thereby the complex will be derailed.

This work has shown that *Ptt*MAP20 shows a high transcript level during secondary cell wall formation and that it associates with the cytoskeletal network. The protein also binds to a cellulose biosynthesis inhibitor, DCB, suggesting relevance for cellulose biosynthesis. The characteristic features of *Ptt*MAP20 suggest a strong connection to cellulose biosynthesis in poplar secondary cell walls, known to have an organized cellulose orientation and cortical microtubuli. The work accomplished in this thesis has led to different hypotheses, described and illustrated in Figure 8 that will hopefully inspire more research efforts directed in solving the molecular function of *Ptt*MAP20 completely.

LIST OF ABBREVIATIONS

Blast - basic local alignment tool

BMT - bovine microtubule

BSA - bovine serum albumin

BY-2 - cultivar Bright Yellow - 2 of the tobacco

cDNA - complementary DNA

CesA - cellulose synthase enzyme

CFP - cyanine fluorescent protein

CS - cellulase synthase complex

Csl - cellulose synthase-like

CSR - class specific region

DCB - 2,6-dichlorobenzonitrile

DCPA - 2,6-dichlorophenylazide

DNA - deoxyribonucleic acid

DP - degree of polymerization

EST - expressed sequence tag

FPLC - Fast performance liquid chromatography

GFP - green fluorescent protein

GH - glycosyl hydrolase

GPI - glycosyl phosphatidylinositol

GT - glucosyltransferase

HEPES - 4-(2-hydroxyethyl)-1-piperazineethanesulfonic acid

HMM - hidden Markov models

HVR - hyper variable region

IMAC - immobilized metal affinity chromatography

IPTG - isopropyl-beta-D-thiogalactopyranoside

kDa - 1000 Daltons

KOR - KORRIGAN

M20L - MAP20-like

MAP - microtubule associated protein

mRNA - messenger ribonucleic acid

MT - microtubule

Mw - molecular weight

PBS - phosphate buffered saline

PCR - Polymerase chain reaction

PLD - phospholipase D

Pt - Populustremula

Ptt- Populustremula x tremuloides

qPCR - quantitative PCR

RACE - rapid amplification of cDNA ends

RNA - ribonucleic acid

RNAi - RNA interference

RT-PCR - reverse transcriptase PCR

SDS-PAGE - sodium dodecyl sulphate polyacrylamide gel electrophoresis

SuSy - sucrose synthase

TATA - TATA box, DNA sequence, cis-regulatory element

TC - terminal complex

TEM - transmission electron microscopy

TPX2 - targeting protein of kinesin-like protein

UDP - uridine 5'-diphosphate'

UTR - untranslated region

WT - wild type

YFP - yellow fluorescent protein

ACKNOWLEDGEMENT

We thankful to TERACRYST and it's publishing group for preparing this article.

ETHICS APPROVAL AND CONSENT TO PARTICIPATE

Not applicable.

HUMAN AND ANIMAL RIGHTS

No Animals/Humans were used for studies that are base of this research.

CONSENT FOR PUBLICATION

Not applicable.

FUNDING

None.

CONFLICT OF INTEREST

There is no conflict of interest in this paper.

REFERENCES

1. King, J.N., Cartwright, C., Hatton, J. and Yanchuk, A.D. The potential of improving western hemlock pulp and paper quality. I. Genetic control and interrelationships of wood and fibre traits. Can. J. Forest Res. 1998; 28, 863-870.
2. Todorow, M. *Pinuspinaster*as a raw material for the paper industry. Iawa Bulletin. 1984; 5, 85-87.
3. Williams, M.F. Matching wood fiber characteristics to pulp and paper processes and products. Tappi. 1994; 77, 227-233.
4. Valade, J.L. The potential use of larch in the Canadian pulp and paper industry: A review. Pulp & Pap Canada. 1998; 99, 156-159.
5. Comeau, P.G., Wang, J.R. and Letchford, T. Influences of paper birch competition on growth of understory white spruce and subalpine fir following spacing. Can. J. Forest Res. 2003; 33, 1962-1973.
6. Dias, A., Lopes, E., Arroja, L., Capela, I. and Pereria, F. Life cycle assessment of paper production from *Eucalyptus globulus*. Case study of the Portuguese industry. Appita J. 2002; 55, 21-26.
7. Zarges, R.V., Neuman, R.D. and Crist, J.B. Kraft pulp and paper properties of populus clones grown under short rotation intensive culture. Tappi. 1980; 63, 91- 94.
8. Schott, S., Chaussy, D. and Mauret, E. Utilisation of straw for the production of pulp and paper. Pap. Puu-Pap. Tim. 2001; 83, 453-457.
9. Sood, Y.V., Pande, P.C., Tyagi, S., Payra, I., Nisha and Kulkarni, A.G. Quality improvement of paper from bamboo and hardwood furnish through fiber fractionation. J. Sci. .Ind. Res. 2005; 64, 299-305.
10. Gutierrez, A., Baldovin, L., Martin, E. and Martinez, F. Non wood raw materials for pulp and paper making. A review. Afinidad. 2004; 61, 400-410.
11. Gavelin, G. Bagasse as raw material for paper making. SvenskPapperstidning-Nordisk Cellulosa. 1979; 82, 351-352.
12. Bhushan, M.B., Ohtani, Y. and Sameshima, K. Normal pressure pulping of jute, kenaf and mestabast fibers. Sen-I Gakkaishi. 1998; 54, 654-660.
13. Payen, A. Mémoire sur la composition du tissupropre des plantes et du ligneux. Compt. Rend. 1838; 7, 1052-1056.
14. Ronquist, F. and Huelsenbeck, J.P. MrBayes 3: Bayesian phylogenetic inference under mixed models. Bioinformatics. 2003; 19, 1572-1574.
15. Yang, Z. PAML: a program package for phylogenetic analysis by maximum likelihood. Comp. App. Biosci. 1997; 13, 555-556.
16. Slater, G.S. and Birney, E. Automated generation of heuristics for biological sequence

comparison. BMC Bioinfo, 2005; 6:31.

17. Solovyev, V.V. and Shahmuradov, I.A. PromH: Promoters identification using orthologous genomic sequences. Nucleic Acids Res. 2003; 31, 3540-3545.
18. Jareborg, N., Birney, E. and Durbin, R. Comparative analysis of noncoding regions of 77 orthologous mouse and human gene pairs. Genome Res. 1999; 9, 1156-1156.
19. Larsson, M., Graslund, S., Li, Y.B., Brundell, E., Uhlen, M., Hoog, C. and Stahl, S. High-throughput protein expression of cDNA products as a tool in functional genomics. J. Biotech. 2000; 80, 143-157.
20. Uggla, C., Magel, E., Moritz, T. and Sundberg, B. Function and dynamics of auxin and carbohydrates during earlywood/latewood transition in Scots pine. Plant Physiol. 2001; 125, 2029-2039.
21. Hamilton, A.J. and Baulcombe, D.C. A species of small antisense RNA in posttranscriptional gene silencing in plants. Science. 1999; 286, 950-952.
22. Shi, S.R., Chaiwun, B., Young, L., Imam, A., Cote, R.J. and Taylor, C.R. Antigen retrieval using ph 3.5 glycine-HCl buffer or urea solution for immunohistochemical localization of Ki-67. Biotech. Histochem. 1994; 69, 213-215.
23. Hertzberg, M., Aspeborg, H., Schrader, J. andersson, A., Erlandsson, R., Blomqvist, K., Bhalerao, R., Uhlen, M., Teeri, T.T., Lundeberg, J., Sundberg, B., Nilsson, P. and Sandberg, G. A transcriptional roadmap to wood formation. Proc. Natl. Acad. Sci. USA. 2001; 98, 14732-14737.
24. Arabidopsis Genome Initiative. Analysis of the genome sequence of the flowering plant Arabidopsis thaliana. Nature.2000; 408, 796-815.
25. Goff, S.A. A draft sequence of the rice genome (*Oryza sativa* L. ssp. *japonica*) (April, pg 92, 2002). Science. 2005; 309, 879.
26. Goff, S.A., Ricke, D., Lan, T.H., Presting, G., Wang, R.L., Dunn, M., Glazebrook, J., Sessions, A., Oeller, P., Varma, H., Hadley, D., Hutchinson, D., Martin, C., Katagiri, F., Lange, et al. A draft sequence of the rice genome (*Oryza sativa* L. ssp*japonica*). Science. 2002; 296, 92- 100.
27. Noble, M., Lewis, S.A. and Cowan, N.J. The microtubule binding domain of microtubule-associated protein map1b contains a repeated sequence motif unrelated to that of Map2 and Tau. J. Cell Biol. 1989; 109, 3367-3376.
28. Wang, X., Zhu, L., Liu, B.Q., Wang, C., Jin, L.F., Zhao, Q. and Yuan, M. Arabidopsis microtubule-associated protein18 functions in directional cell growth by destabilizing cortical microtubules. Plant Cell. 2007; 19, 877-889.
29. Valentine, T., Shaw, J., Blok, V.C., Phillips, M.S., Oparka, K.J. and Lacomme, C. Efficient virus-induced gene silencing in roots using a modified tobacco rattle virus vector. Plant Physiol. 2004; 136, 3999-4009.

30. Smertenko, A.P., Chang, H.Y., Wagner, V., Kaloriti, D., Fenyk, S., Sonobe, S., Lloyd, C., Hauser, M.T. and Hussey, P.J. The *Arabidopsis* microtubule-associated protein AtMAP65-1: Molecular analysis of its microtubule bundling activity. Plant Cell. 2004; 16, 2035-2047.
31. Wittmann, T., Wilm, M., Karsenti, E. and Vernos, I. TPX2, A novel xenopus MAP involved in spindle pole organization. J. Cell. Biol. 2000; 149, 1405- 1418.
32. Wittmann, T., Boleti, H., Antony, C., Karsenti, E. and Vernos, I. Localization of the kinesin-like protein Xklp2 to spindle poles requires a leucine zipper, a microtubule-associated protein and dynein. J. Cell. Biol. 1998; 143, 673-685.